Elasticity of Semiflexible Polymers with and without Self-Interactions

ARTICLE *in* MACROMOLECULES · JULY 2003

Impact Factor: 5.8 · DOI: 10.1021/ma0348831 · Source: arXiv

4 AUTHORS, INCLUDING:

Trinh Xuan Hoang
Vietnam Academy of Science and Technology
54 PUBLICATIONS **1,093** CITATIONS
SEE PROFILE

Amos Maritan
University of Padova
308 PUBLICATIONS **9,211** CITATIONS
SEE PROFILE

Elasticity of semiflexible polymers with and without self-interactions

A. Rosa[1], T. X. Hoang[2], D. Marenduzzo[3], A. Maritan[1,2]
[1] *International School for Advanced Studies (SISSA) and INFM, Via Beirut 2-4, 34014 Trieste, Italy*
[2] *The Abdus Salam International Center for Theoretical Physics (ICTP), Strada Costiera 11, 34100 Trieste, Italy*
[3] *Department of Physics, Theoretical Physics, University of Oxford, 1 Keble Road, Oxford OX1 3NP, England*

A *new* formula for the force vs extension relation is derived from the discrete version of the so called *worm like chain* model. This formula correctly fits some recent experimental data on polymer stretching and some numerical simulations with pairwise repulsive potentials. For a more realistic Lennard-Jones potential the agreement with simulations is found to be good when the temperature is above the θ temperature. For lower temperatures a plateau emerges, as predicted by some recent experimental and theoretical results, and our formula gives good results only in the high force regime. We briefly discuss how other kinds of self-interactions are expected to affect the elasticity of the polymer.

PACS numbers:

I. INTRODUCTION

The behaviour of a single polymeric molecule under stretching has become a popular subject among experimental physicists (see e.g. [1], for a review) and has attracted the attention of theoreticians who have introduced several models to explain these results. An exhaustive description on this topic is hard to achieve within a single model, since the experimental conditions strongly affect the results. So, the most common theoretical approaches are usually only a first step approximation.

Here, we focus our attention mainly on the pulling of a polymer under good solvent conditions [2], in which case we give an analytical prediction for the force versus extension curve. We also discuss other cases by means of numerical simulations and direct connections to experiments. Usually, the models adopted describe the polymer as an elastic (ideal) chain, where self-avoidance is not taken into account. Typically, freely jointed (FJC) or worm like chain (WLC) are studied [3].

The former describes a chain of beads connected by links of constant distance, whereas the latter introduces an intrinsic *stiffness* between two consecutive bonds and, in particular, is shown to correctly describe a wide range of experimental results on double-stranded (ds) DNA, single plasmid and lambda phage DNA [4–6]. In this case, the large force behaviour $1-z/L_c \sim 1/\sqrt{F}$ is found, where z is the elongation along the direction of the force, L_c the contour length of the polymer and F is the applied force [4, 7]. Let us note that in these cases the *continuous* version of the WLC model is always used, where the *persistence* length [4] L_p is very large, compared to the base separation (roughly one persistence length is 150 base pairs).

Here, we focus on the *discrete* version of the WLC model, that satisfactorily describes the pulling behaviour of a polymer in good solvent. We broadly identify three regimes in the force vs extension curves obtained in our analytical and numerical calculations. The low force (or low stretch) regime is highly affected by the details of the interactions between the beads (which in nature are, e.g., caused by the different concentration of ions in solution). This regime is discussed only marginally here, as, though it is potentially very interesting, experimental data in the range of forces are quite rare and not precise enough to allow a comparison with theoretical predictions. There is then a second regime, of intermediate stretches or forces, in which the force versus extension characteristic curves obey approximately the laws predicted a few years ago in Ref. [4] by means of a continuum theory of the WLC. Finally, for very large forces (beyond a polymer dependent crossover value), we get a universal, model-independent, freely-jointed-chain like behaviour. In Section II, we introduce the discrete WLC model and show how it can be related to the well known continuous version. In Section III, we show a comparison between our theory and some recent experiments. Then, in Sections IV and V, we introduce some extension vs force curves obtained from Monte-Carlo and Molecular Dynamics calculations for models of stiff and flexible polymers with a chosen potential between *non* nearest neighbour beads. We shall consider two different cases: a pure repulsive potential and a more realistic Lennard-Jones potential and we show that in the latter case our formula agrees with the numerical data only in the case of high temperatures or, for lower temperatures in the high force regime. Below the θ point a force plateau appears, as predicted by some recent theoretical works [8–11] and confirmed by experiments [5]. Finally, Sections VI and VII are left for discussion and conclusions, respectively.

II. THE MODEL

Our model describes a chain of beads, where the distance between the nearest neighbours is kept fixed (we can put it equal to b) and a suitable *stiffness* K is introduced. Then, the corresponding Boltzmann weight reads [12–14]:

$$e^{-\beta\mathcal{H}} = \prod_{i=1}^{N} \delta(|\mathbf{t}_i| - b) e^{\beta K \sum_{i=1}^{N} \mathbf{t}_i \mathbf{t}_{i+1} + \beta \mathbf{F} \sum_{i=1}^{N} \mathbf{t}_i}, \quad (1)$$

where $\beta = 1/T$, T being the temperature in units of Boltzmann constant, $\mathbf{t}_i \equiv \mathbf{r}_i - \mathbf{r}_{i-1}$ ($\mathbf{r}_i$ being the position vector for the i-th bead, $i = 1, ..., N$ and N is the total number of beads) and $\mathbf{F}$ is the applied force which defines the z-direction. The partition function for the model described by (1) is

$$\mathcal{Z}_N = \int \prod_{i=1}^{N} d\mathbf{t}_i e^{-\beta\mathcal{H}}. \quad (2)$$

The average elongation $\langle z \rangle_N$ along the stretching direction is

$$\langle z \rangle_N = T \frac{\partial}{\partial F} \log \mathcal{Z}_N. \quad (3)$$

In the thermodynamic limit ($N \to \infty$), the large force behaviour of Eq. (3) gives

$$\zeta \equiv \lim_{N\to\infty} \frac{\langle z \rangle_N}{Nb} = 1 - \frac{T}{\sqrt{(bF)^2 + 4bKF}}. \quad (4)$$

The continuum approximation of Eq. (4) is obtained with the following substitutions [15]:

$$\beta K \to L_p/b, \quad (5)$$

in the formal limit $b \to 0$, where L_p is the persistence length. The final result $\zeta = 1 - 1/2\sqrt{\beta L_p F}$ does agree with the celebrated result of Marko and Siggia [4]. However, our result is more general, since it predicts a *crossover* force $F_c = \frac{4L_p}{\beta b^2}$:

$$\begin{array}{ll} \text{WLC-like behaviour:} & 1 - \zeta \sim 1/\sqrt{F}, \quad F \ll F_c \\ \text{FJC-like behaviour:} & 1 - \zeta \sim 1/F, \quad F \gg F_c \end{array}. \quad (6)$$

Let us notice that the validity of the continuum approximation proposed in Ref. [4] is not simply related to the value of the dimensionless ratio b/L_p but rather to F/F_c.

From Eq. (4), we deduce that:

$$\beta b F = \frac{2L_p}{b} \left[\sqrt{1 + \left(\frac{b}{2L_p}\right)^2 \frac{1}{(1-\zeta)^2}} - 1 \right]. \quad (7)$$

The low force behaviour of Eq. (3) is

$$\zeta = \frac{\beta b F}{3} \frac{1 + y(L_p/b)}{1 - y(L_p/b)}, \quad (8)$$

where $y(x) = \coth(x) - 1/x$ [16]. Again, in the limit $b \to 0$, Eq. (8) agrees with the result of Marko and Siggia [4]. Matching Eqs. (7) and (8), we obtain the following interpolation formula:

$$\begin{aligned} \beta b F \;=\; & \frac{2L_p}{b} \left[\sqrt{1 + \left(\frac{b}{2L_p}\right)^2 \frac{1}{(1-\zeta)^2}} - \sqrt{1 + \left(\frac{b}{2L_p}\right)^2} \right] \\ & + \left(3 \frac{1 - y(L_p/b)}{1 + y(L_p/b)} - \frac{b/2L_p}{\sqrt{1 + (b/2L_p)^2}} \right) \zeta. \end{aligned} \quad (9)$$

It is easy to verify that Eq. (9) correctly reproduces the right large and small force behaviours, Eqs. (7) and (8) and that in the *continuum* limit $b \to 0$ we obtain the well known interpolation formula [4]:

$$\beta L_p F = \frac{1}{4(1-\zeta)^2} - \frac{1}{4} + \zeta. \quad (10)$$

In next Section, we shall apply our formula, Eq. (9), to two recent experiments. The first discusses the stretching of a single plasmid DNA molecules, to which the formula (10) was previously applied with success [5]. Nevertheless, our formula predicts a non trivial value for the parameter b, that gives an estimate for the *intra* bead distance. Then, the second experiment [17, 18] demonstrates that Eq. (9) gives the right large force behaviour.

In the following, we shall define $\zeta = z/L_c$, where z is the elongation along the direction of the force and $L_c = Nb$ is the contour length of the polymer (see also Eq. (4)).

III. COMPARISON WITH TWO RECENT EXPERIMENTS

Let us consider the experimental data reported in the plot at the top of Fig. 3 of Ref. [5]. The authors considered the elastic response of a single plasmid of DNA molecules, probed using optical tweezers [19]. They found that, according to the environmental conditions, it can be very different. In particular, for condensed molecules, the stretching curves display a stick-release pattern, where the DNA molecule can be described as a succession of different WLC's of different contour and persistence lengths. We are mainly interested to the case of uncondensed molecules, whose stretching pattern is reproduced in Fig. 1.

As described in the caption, the contour and persistence lengths obtained with our formula, Eq. (9), and with Eq. (10) are perfectly compatible. Nevertheless Eq. (9) predicts a non trivial value for the intra bead effective distance $b = 2.5$ nm, that corresponds to $7 - 8$ base pairs. Let us notice that this matches the DNA hydration thickness (here, we have used ~ 0.34 nm as the distance between two consecutive base pairs [5]).

If we take $T = 300$ K, the crossover force $F_c \sim 100$ pN and $F/F_c \lesssim 0.16$ for the data of Ref. [5], thus justifying the use of the interpolation formula, Eq. (10).

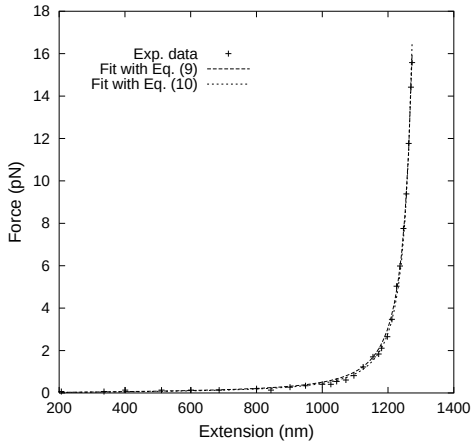

FIG. 1: (+): experimental data taken from Ref. [5]. Long dashed line: fit with the curve, Eq. (9), yielding $L_c = 1324$ nm, $L_p = 38$ nm and $b = 2.5$ nm. Short dashed line: fit with the curve, Eq. (10), yielding $L_c = 1324$ nm and $L_p = 38$ nm, see Ref. [5].

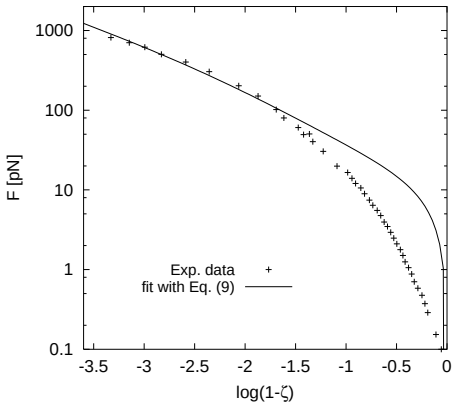

FIG. 2: (+): experimental data taken from Ref. [18]. Continuous line: fit with the curve, Eq. (9), yielding $L_c = 2.31$ (in units of the contour length l^0_{ds} of the equivalent dsDNA molecule observed in 10 mM PB [18]), $L_p = 0.26$ nm and $b = 0.12$ nm.

However, as pointed out in Eq. (6), the discrete nature of the chain does emerge, when $F \gtrsim F_c$. Notice also that for forces considerably smaller than F_c double-stranded DNA would undergo an overstretching transition [20], where a more sophisticated theory is needed [3].

An interesting question is how this treatment may be applied to single-stranded DNA (ssDNA). On one hand, if we keep as physical parameters the persistence length of ssDNA ~ 1 nm, and as the equivalent of b the separation between two phosphates, i.e. 0.5 nm roughly, we would end up with a crossover force again of the order of 70 pN. Data in this regime do exist [17, 18], and suggest that the WLC grossly fails to fit the data [18, 21]. In fact (see Fig. 4, Ref. [18]), the authors pointed out that the corresponding fit with Eq. 10 gives good results in the large force regime, but with a calculated persistence length ($\simeq 0.21$ nm) which is clearly *not* physical. Our equation does not do much better for low and intermediate force, in which case, as shown in Ref. [18], evidently the self-interactions dominate the behaviour. Still a large force fit, even if a bit dependent on the contour length which we choose, suggests that the large force exponent in the $(\log(1-\zeta), \log(F))$ plane is -1 as predicted by our model (see Fig. 2). The calculated fitting parameters L_p and b (see the caption of Fig. 2) give $F_c \simeq 300$ pN, which is consistent with our Eq. (9) (see Fig. 2).

In next Section we introduce some Monte-Carlo calculations and compare them to Eqs. (9) and (10).

IV. MONTE-CARLO CALCULATIONS

As already said, our model is a *stiff* chain described by the Boltzmann weight, Eq. (1), where the *intra* bead distance b is now kept fixed to 1.

In Fig. 3 we have plotted the Monte-Carlo data (+)

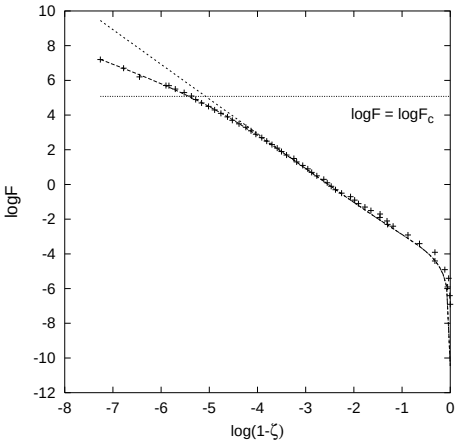

FIG. 3: (+): Monte-Carlo data for a *stiff* chain of $N = 100$ beads and stiffness $K = 40$, for $\beta = 1$. Long dashed line: Eq. (9) with $L_p = 40$ and $b = 1$. Short dashed line: Eq. (10) with $L_p = 40$. The *crossover* force F_c, see Eq. (6), is also shown.

and the curves given by Eqs. (9) and (10) (long and short dashed line, respectively), for $L_p = 40$, and $\beta = 1$. As observed, the agreement is perfect only for Eq. (9). In fact, the discrete nature of the chain emerges around $F = F_c \sim 160$ (in the chosen units) and the WLC approximation is no more valid.

To render the model more realistic, let us introduce a *short* range repulsive potential $V_{rep}(r)$ between non consecutive nearest neighbour beads. We have adopted the following functional form:

$$V_{rep}(r) = \frac{1}{r^{12}} \tag{11}$$

where r is the distance between two beads. Then, we

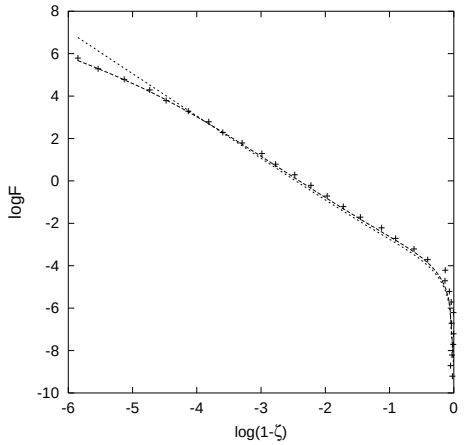

FIG. 4: (+): Monte-Carlo data for a *stiff* chain of $N = 100$ beads, stiffness $K = 30$ and interaction potential given by Eq. (11), for $\beta = 1$. Long dashed line: fit obtained from Eq. (9) with $L_p \simeq 31$ ($b = 1$). Short dashed line: fit obtained from Eq. (10) with $L_p \simeq 34.9$.

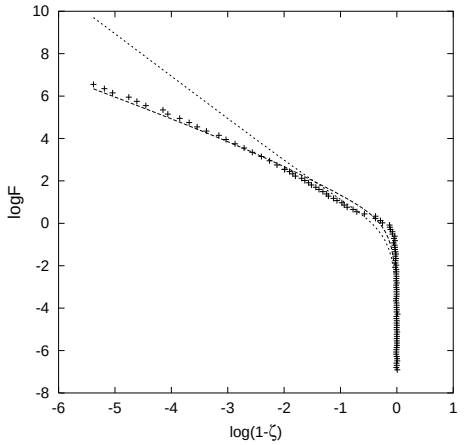

FIG. 5: (+): Monte-Carlo data for a *stiff* chain of $N = 100$ beads, stiffness $K = 10$ and interaction potential given by Eq. (13), for $\beta = 0.3$. Long dashed line: fit obtained from Eq. (9) with $L_p \simeq 2.12$, $b \simeq 1.26$. Short dashed line: fit obtained from Eq. (10) with $L_p \simeq 2.41$.

have to multiply the Boltzmann weight, Eq. (1), by

$$e^{-\frac{\beta}{2}\sum_{i\neq j=0}^{N} V_{rep}(r_{ij})} \tag{12}$$

where we have defined $r_{ij} = |\mathbf{r}_i - \mathbf{r}_j|$.

In Fig. 4 we have plotted the Monte-Carlo results (+) for $K = 30$, together with the two fitting lines obtained from Eqs. (9) and (10) (long and short dashed lines, respectively). The corresponding persistence lengths are $L_p \simeq 31$ (b is kept fixed to 1) and $L_p \simeq 34.9$. Again, we can observe that our formula works better than Eq. (10). Moreover, this last result is in agreement with some theoretical works [22, 23], that predicts that the net effect of the repulsive potential is to renormalize the persistence length, making it larger than the bare one.

Now, let us introduce a more realistic potential, adding to the repulsive core an attractive part too. It is interesting to notice that the approaches of Refs. [22, 23] can not be generalized, since the attractive part introduces some instabilities and the perturbation scheme discussed there is no more valid.

We have chosen the following Lennard-Jones kind functional form $V_{LJ}(r)$:

$$V_{LJ}(r) = V_0 \left(\frac{1}{r^{12}} - \frac{\alpha}{r^6} \right). \tag{13}$$

The parameters V_0 and α are chosen in such a way that the minimum of the energy is located at $r = r_{min} = 1.5$ and $V_{LJ}(r = r_{min}) = -1$. We expect that Eq. (10) does not work well in this case. Our goal is to test our formula, Eq. (9).

Firstly, we show the effects of increasing stiffness on the force vs extension curves. To fix the ideas, we begin to consider a sufficiently high temperature, i.e. *above* the θ point [2, 16], whose location, however, is not exactly known. In Ref. [24], the authors were able to numerically determine the θ temperature T_θ for a model of homopolymer with a square well potential, whose depth is fixed to -1. They found that $T_\theta \simeq 3$. Our T_θ should be somewhat smaller due to the stiffness.

Initially, we fix $\beta = 0.3$ ($T = 3.333...$), with $K = 10$. The numerical results and the corresponding fitting line are plotted in Fig. 5. The corresponding fitting parameters are described in the caption. In this case we allowed b to be a free parameter and we have determined it through a best fit of the data even though in the simulated model $b = 1$. The fit with our formula is surprisingly good, in contrast with the result obtained with Eq. (10). Moreover, the predicted value for b is of the correct order. This means that the effect of the stiffness compensates the attraction due to the potential and the behaviour is similar to a FJC. Let us stress on the fact that if we fix $b = 1$, the corresponding fits are considerably less precise.

We have also simulated the case with $K = 80$. In Fig. 6 we have plotted the numerical data together with the two fitting lines (the fitting parameters are reported in the caption). The agreement with our formula is again perfect, in contrast with Eq. (10).

For both situations plotted in Figs. 5 and 6, we note that the main effect due to the potential is a considerable reduction in the persistence length due to the attractive part, which evidently renormalize also the intra bead distance.

As a check, let us notice that the correlation function $\langle \mathbf{t}_i \cdot \mathbf{t}_{i+r} \rangle$ for the WLC is [16]:

$$\langle \mathbf{t}_i \cdot \mathbf{t}_{i+r} \rangle = y(\beta K)^r, \tag{14}$$

where the function $y(x)$ has been defined above. In the continuum limit

$$\langle \mathbf{t}_i \cdot \mathbf{t}_{i+r} \rangle = \exp(-r/L_p). \tag{15}$$

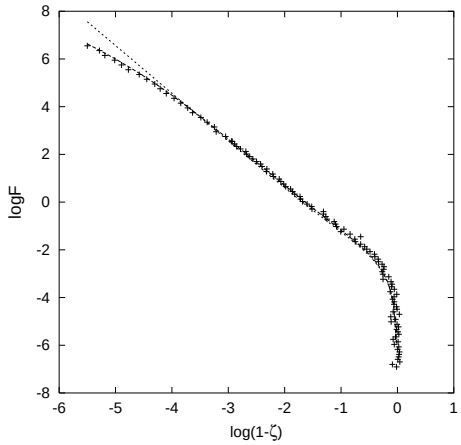

FIG. 6: (+): Monte-Carlo data for a *stiff* chain of $N = 100$ beads, stiffness $K = 80$ and interaction potential given by Eq. (13), for $\beta = 0.3$. Long dashed line: fit obtained from Eq. (9) with $L_p \simeq 23.33$ and $b = 0.86$. Short dashed line: fit obtained from Eq. (10) with $L_p \simeq 25.95$.

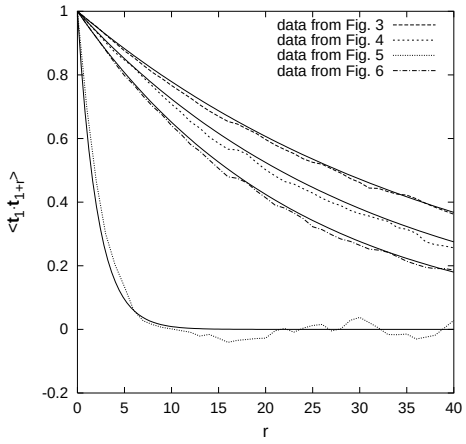

FIG. 7: Plot of the correlation functions $\langle \mathbf{t}_1 \cdot \mathbf{t}_{1+r} \rangle$ vs r, calculated from the data of Figs. 3 to 6 and the corresponding theoretical predictions (continuous lines), given by Eq. (15).

This result is exact for all r but holds in a more general context, like the case with interaction, in the large r limit. In Fig. 7 we have plotted the correlation functions $\langle \mathbf{t}_1 \cdot \mathbf{t}_{1+r} \rangle$ vs r for the data of Figs. 3 to 6 and compared them to the theoretical ones as given by Eq. (15). The corresponding persistence lengths are those found with our formula. The agreement is perfect.

Let us now consider the case of $\beta = 0.5$ ($T = 2$). In Fig. 8 we have plotted the case for $K = 10$. As it can be seen a *first order* phase transition emerges [9, 25]. In this case our formula is able to describe only the part of the plot at relatively large forces.

A complete characterization of the force vs extension behaviour in this case needs a more complete theory and is beyond the scopes of this work. We reserve to study this important issue in a future work (see also Ref. [26] for some recent Monte-Carlo results about stiff polymers).

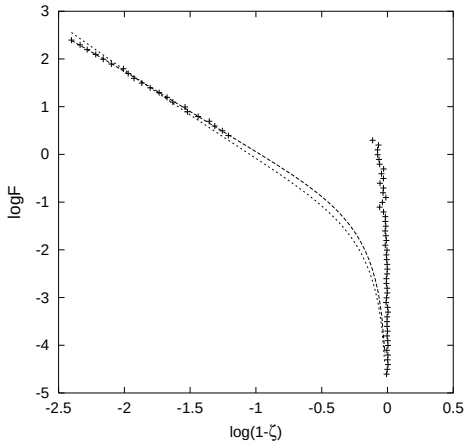

FIG. 8: (+): Monte-Carlo data for a *stiff* chain of $N = 100$ beads, stiffness $K = 10$ and interaction potential given by Eq. (13), for $\beta = 0.5$. Long dashed line: fit obtained from Eq. (9) with $L_p \simeq 4.42$ and $b = 1.03$. Short dashed line: fit obtained from Eq. (10) with $L_p \simeq 4.85$. Let us remark that we have tried to fit only the range of data at large forces.

V. MOLECULAR DYNAMICS CALCULATIONS

In the Monte-Carlo simulations presented in previous Section we were working in fixed force ensembles, i.e. the force was fixed in each simulation and the averaged extension of the chain was computed. It is interesting to check if in fixed stretch ensembles, i.e. when one fixes the extension and measures the averaged force, the results remain unaltered. In the following we will present and discuss Molecular Dynamics (MD) simulation results in which we can perform a quasi-fixed stretch treatment. In these simulations (similar to what has been done for protein-like polymers [27, 28]) the two ends of the polymer are tethered by springs to two fixed points in space so its end-to-end vector can vary only little. The two fixed points are chosen such that a line connecting them is along the z-direction. We will consider two cases: a) when there are repulsions between two non-consecutive beads and b) when the beads interact via a Lennard-Jones (LJ) potential. Note that we do not include the intrinsic stiffness into the models considered in this Section (i.e. $K = 0$).

Our homopolymers are modeled as chains of beads connected by springs. The harmonic potential for the chain connectivity reads

$$V_{i,i+1} = \frac{1}{2} k (r_{i,i+1} - b)^2 \,, \tag{16}$$

where $r_{i,i+1} = |\mathbf{r}_i - \mathbf{r}_{i+1}|$ is the distance between two consecutive beads. b is fixed to 1 and $k = 1444\epsilon$ is the chosen spring constant (ϵ is a unit of energy). We use

the same spring constant k for the potential that tethers the ending beads to the fixed points. For the case of repulsion the following potential is used

$$V_{i,j} = \epsilon \left(\frac{\sigma}{r_{ij}} \right)^{12} \quad , \tag{17}$$

where $\sigma = 1.32$. For the case of attraction the LJ potential takes the form

$$V_{i,j} = 4\epsilon \left[\left(\frac{\sigma}{r_{ij}} \right)^{12} - \left(\frac{\sigma}{r_{ij}} \right)^{6} \right] . \tag{18}$$

The model is studied by a MD method in which coupling to the heat bath is provided by the Langevin equation (see e.g. Ref. [27] for details). In the following temperature will be given in units of ϵ/k_B where k_B is the Boltzmann constant. We consider chains of 60 residues and simulations are done for various temperatures. The averaged force $\langle F \rangle$ exerted on each of the fixed points and the averaged z-component of the end-to-end vector of the chain $\langle z \rangle$ are measured under equilibrium condition at a constant temperature. As we vary the position of one fixed point versus the other we are able to obtain $\langle F \rangle$ vs $\langle z \rangle$ under a quasi-fixed stretch condition (the fluctuation in z is considerably small).

It should be noted that due to the springs used for the chain connectivity the contour length L_c is not a constant as one varies the stretching distance. We find that as the polymer approaches its full extension L_c may increase up to 5-10% depending on the temperature. We find that however if the relative extension ζ is defined as $\langle z \rangle / \langle L_c \rangle$, where $\langle L_c \rangle$ is the averaged contour length computed from the simulations at a given stretch z, then the $\langle F \rangle$ vs ζ acquires very little changes as we increase k by a factor of 2 or 3.

In Fig. 9 we show the stretching data for the chain with repulsive potential given by Eq. (17) at $T = 1$ (at some other temperatures we found that the results are qualitatively similar). One can see that the data can be fitted quite well by Eq. (9) at high extension, but not at low extension. The least-squared fit to the data gives $b \simeq 1.05$ and $L_p \simeq 1.04$. Note that the value of b obtained from the fit is reasonably good though it is somewhat larger than the bond length when no tension is applied. This increment (of about 5%) however is in a good agreement with the increase in L_c under stretching and can be understood as due to the softness of the bond's potential. Thus Eq. (9) still gives the right physics. One can also notice that our homopolymer with repulsive potentials corresponds to a worm-like chain with a low stiffness ($L_p \simeq b$). We have computed directly the persistence length from the correlation $\langle \mathbf{t}_i \cdot \mathbf{t}_{i+r} \rangle$ by performing simulations for a free chain and found that L_p is approximately 2.35 at $T = 1$. The difference (of a factor of 2) between the measured persistence length and the one obtained from the fit is due to the fact that the fit was good only at a high extension. In this regime the excluded volume effects are much smaller than in a free chain, thus resulting in a lower persistence length. It should be noted that Marko and Siggia's formula (Eq. (10)) completely fails to fit the data. This is related to the fact that for chains with low stiffness the continuum limit $b \to 0$ cannot be applied and the discreteness of the chain should be taken into account.

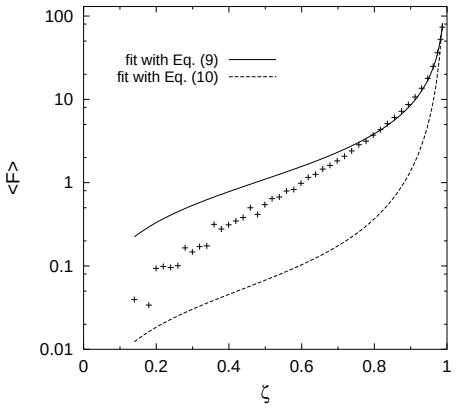

FIG. 9: Force $\langle F \rangle$ vs relative extension ζ for a 60-bead chain with repulsion studied by Molecular Dynamics simulations under quasi-fixed stretch conditions (see text). ζ is defined as $\langle z \rangle / \langle L_c \rangle$ where $\langle z \rangle$ and $\langle L_c \rangle$ are the averaged extension and the averaged contour length obtained in the simulation. The data points shown are for temperature $T = 1$. The fit to Eq. (9) (solid line) yields $b \simeq 1.05$ and $L_p \simeq 1.04$. Eq. (10) fails to fit the data (dashed line).

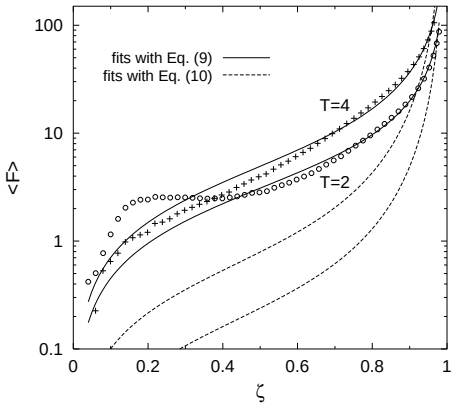

FIG. 10: Force $\langle F \rangle$ vs relative extension ζ for chain with Lennard-Jones (LJ) potentials under quasi-fixed stretch conditions. The fits of the data to Eq. (9) (solid lines) yield $b \simeq 1.01$ and $L_p \simeq 0.88$ for $T = 4$, and $b \simeq 1.0$ and $L_p \simeq 0.5$ for $T = 2$. Eq. (10) fails to fit the data at both temperatures (dashed lines).

We turn now to discuss our results for homopolymers with attraction. Fig. 10 shows the force vs relative extension for a 60-bead chain with the Lennard-Jones potential given by Eq. (18). We find that Eq. (9) can reasonably fit the data for temperatures higher than the

collapse transition temperature T_θ whereas at lower temperatures it can fit the data only at high extension. The T_θ temperature is estimated to be between 2 and 3 for this system. As shown in Fig. 10 at $T = 4$ Eq. (9) appears to fit both high and low extension data yielding $b \simeq 1.01$ and $L_p \simeq 0.88$. At $T = 2$ the fit can be given only at large extension, which yields $b \simeq 1.0$ and $L_p \simeq 0.5$. Note that at both temperatures the value of b obtained from the fits is quite consistent with the correct bond length. Like for the case of repulsion, due to the low stiffness induced by the potentials, the Marko and Siggia formula does not fit the data as our new formula does.

It should be noted that when the temperature is about the collapse transition temperature T_θ we observe a *plateau* in the force vs extension (see the case of $T = 2$ in Fig. 10), similar to what seen in the previous Section. However, at temperatures lower than T_θ, in the fixed stretch ensemble the force vs extension curve shows the typical behaviour with hysteresis phenomenon [27, 28].

VI. DISCUSSION

Though our main results refer to a situation in which attractive interactions are not very important, it is useful to further comment on how our results change in the presence of such a situation in a real experiment. Such attractions change the picture depicted so far as, if they are strong enough, they can cause a phase transition in the molecule.

An effective self-attraction, like the one considered here by means of a $6-12$ Lennard-Jones potential, arises due to hydrophobic interactions in polypeptides and due to a suitably large concentration of polyvalent counterions in the case of double-stranded DNA. If this is the case, the polymer is in poor solvent conditions or equivalently below the θ point (in the nomenclature of the models discussed above). In these cases at zero stretch the force attains (in a thermodynamically long chain) a non-zero value followed by a force plateau for long molecules [9]. This indicates the presence of a first order transition. We have already seen in the previous section that in this situation (i.e. in poor solvent conditions) the two ensembles, fixed force and fixed stretch, are not equivalent and indeed in the experiments the stretching curves of small DNA's or of DNA's in presence of a high concentration of polyvalent counterions in reality show peaks. A thorough explanation of this effect includes polyelectrolyte modeling, finite size corrections as well as dynamical effects and can be found in Refs. [9, 10].

A different scenario holds for ssDNA and for RNA (this scenario would also be retraced if a self-attractive polymer such as dsDNA in presence of condensing agents is restricted conformationally to stay in a quasi-two-dimensional film). In these cases the single molecule phase transition is second order and thus at low stretch the characteristic force curves are non-zero and then rise smoothly. Furthermore, the attraction in ssDNA and RNA is brought forth by the base pairing interactions between bases far apart in the chain. If sequence disorder is neglected, the low force regime can be written as follows:

$$\zeta \sim (f - f_c)^{1/\Delta - 1} \tag{19}$$

where f_c is the critical force. The exponent Δ is between 0.5 (the value of native branched polymer-like configurations arising from base stacking [29]) and 1 (for a polymer in a good solvent). While present day experiments show that as the extension goes to 0 the force is non-zero [30], the data are not clean enough to allow discriminating between the exponents above. To be noted that within a simplified theory [30], it was possible to find a law implying $\Delta = 1/2$.

VII. CONCLUSIONS

Here, we have revised the well known WLC model that correctly describes the behaviour under pulling of a *stiff* polymer. We have pointed out that its discrete version has a different large force behaviour respect to the continuous version by Marko and Siggia [4], Eq. (6). We predict a *crossover* force between these two different regimes. It should be noticed that a recent paper by Livadaru et al. [31] reports a similar result. However, here we have given a simpler formula, Eq. (9), which can be tested on real polymers as well as on numerical simulations, where self-interactions are present.

So, firstly, we have used it to fit some experimental data on dsDNA, Fig. 1, and ssDNA, Fig. 2. In the former case, where Eq. (10) was already applied with success, we find that Eq. (9) predicts a not trivial intra bead distance and a crossover force, which is much greater than the experimental forces. This justifies the approach by Marko and Siggia. In the latter case, we observe a clear crossover between the two regimes. In fact, now the crossover force is small and the assumption leading to Eq. (10) is no longer justified.

Then, we have performed some Monte-Carlo simulations to verify the validity of our formula. We have analyzed different kinds of intra bead potentials. For a short range *repulsive* potential we have correctly found that our formula is in good agreement with the numerical data, predicting a renormalized stiffness [22, 23]. For a more realistic Lennard-Jones potential the situation is more complicated. For temperatures above the θ point, Eq. (9) gives a good fit. The main result is that, now, both the persistence length and the intra bead distance b are renormalized by the potential. For temperatures below the θ point, our formula agrees with the numerical data only at large forces.

We have performed also simulations to examine the validity of our new formula for the pulling of flexible polymers under quasi-fixed stretch conditions. This kind of simulations has been done by using Molecular Dynamics

methods. Like in Monte-Carlo simulations we considered chains with repulsive and attractive Lennard-Jones potentials but now the chains have no intrinsic stiffness. It is found that for both types of interaction our new formula works very well at high extension and it correctly predicts the intra bead distance. The case of attraction is even more interesting since when the temperature is above the θ point both the the high and low extension stretching data can be fitted reasonably well to Eq. (9). It is shown that the Marko and Siggia formula does not fit the numerical data for the chains considered. The reason for this is that the modest stiffness induced by the Lennard-Jones potentials is not sufficiently large to yield the continuous WLC behaviour as described by Eq. (10). The results indicate that Eq. (9) can be used to characterize elastic behaviours of a much wider range of biomolecules.

Finally, we have discussed how an attractive potential can modify the pulling behaviour of a polymer under poor solvent conditions.

VIII. ACKNOWLEDGMENTS

We thank F. Seno and C. Micheletti for illuminating discussions.

[1] C. Bustamante, J. C. Macosko, G. J. L. Wuite, *Nat. Rev. Mol. Cell. Bio.* **1**, 130 (2000).
[2] P.-G. De Gennes, *Scaling Concepts in Polymer Physics* (Cornell University Press, Ithaca, 1979).
[3] M. D. Wang, H. Yin, R. Landick, J. Gelles, S. M. Block, *Biophys. J.* **72**, 1997 (2000).
[4] J. F. Marko, E. D. Siggia, *Macromolecules* **28**, 8759 (1995).
[5] C. G. Baumann, V. A. Bloomfield, S. B. Smith, C. Bustamante, M. D. Wang, *Biophys. J.* **78**, 1965 (2000).
[6] R. Podgornik, P. L. Hansen, V. A. Parsegian, *J. Chem. Phys.* **113**, 9343 (2000).
[7] A. Lamura, T. W. Burkhardt, G. Gompper, *Phys. Rev. E* **64**, 061801 (2001).
[8] A. Halperin, E. B. Zhulina, *Europhys. Lett.* **15**, 417 (1991).
[9] D. Marenduzzo, A. Maritan, A. Rosa, F. Seno, *Phys. Rev. Lett.* **90**, 088301 (2003).
[10] Y. Murayama, Y. Sakamaki, M. Sano, *Phys. Rev. Lett.* **90**, 018102 (2003).
[11] N. K. Lee, T. A. Vilgis, *Eur. Phys. J. B* **28**, 451 (2002).
[12] M. Fixman, J. Kovac, *J. Chem. Phys.* **58**, 1564 (1973).
[13] S. Cocco, R. Monasson, J. F. Marko, *Phys. Rev. E* **66**, 051914 (2002).
[14] S. Cocco, J. F. Marko, R. Monasson, *Cr. Phys.* **3**, 569 (2002).
[15] D. Bensimon, D. Dohmi, M. Mezard, *Europhys. Lett.* **42**, 97 (1998).
[16] M. Doi, S.F. Edwards, *The Theory of Polymer Dynamics* (Clarendon Press, Oxford, 1988).
[17] M. Rief, H. Clausen-Schaumann, H. E. Gaub, *Nat. Struct. Biol.* **6**, 346 (1999).
[18] M.-N. Dessinges, B. Maier, Y. Zhang, M. Peliti, D. Bensimon, V. Croquette, *Phys. Rev. Lett.* **89**, 248102 (2002).
[19] U. Bockelmann, Ph. Thomen, B. Essavez-Roulet, V. Viasnoff, F. Heslot, *Biophys. J.* **82**, 1537 (2002).
[20] S. B. Smith, Y. Cui, C. Bustamante, *Science* **271**, 795 (1996).
[21] A. Montanari, M. Mézard, *Phys. Rev. Lett.* **86**, 2178 (2001).
[22] N. Lee, D. Thirumalai, *Eur. Phys. J. B* **12**, 599 (1999).
[23] P. L. Hansen, R. Podgornik, *J. Chem. Phys.* **114**, 8637 (2001).
[24] Y. Zhou, C. K. Hall, M. Karplus, *Phys. Rev. Lett.* **77**, 2822 (1996).
[25] A. Rosa, D. Marenduzzo, A. Maritan, F. Seno, *Phys. Rev. E* **67**, 041802 (2003).
[26] D. A. Kessler, Y. Rabin, cond-mat/0302505.
[27] M. Cieplak, T. X. Hoang, M. O. Robbins, *Proteins* **49**, 104 (2002).
[28] M. Cieplak, T. X. Hoang, M. O. Robbins, *Proteins* **49**, 114 (2002).
[29] G. Parisi, N. Sourlas, *Phys. Rev. Lett.* **46**, 871 (1981).
[30] A. V. Tkachenko, cond-mat/0304250.
[31] L. Livadaru, R. R. Netz, H. J. Kreuzer, *Macromolecules* **36**, 3732 (2003).